Microstructure and Mechanical Properties of the Friction Welded Joint between X53CrMnNiN219 and X45CrSi93 Stainless Steel

M.R. Abbassi[1], Kh. Gheisari [1*]

[1] *Department of Materials Science and Engineering, Faculty of Engineering, Shahid Chamran University of Ahvaz, Ahvaz, Iran*

ARTICLE INFO

Article history:

Received 2 July 2016
Accepted 2 December 2016
Available online 15 March 2017

Keywords:

Dissimilar metals welding
Heat treatment
Upset zone
X53CrMnNiN219 austenitic stainless steel
X45CrSi93 martensitic stainless steel

ABSTRACT

Dissimilar metals friction welding of austenitic–martensitic stainless steels is commonly used for manufacturing engine valves in automobile industry. In this study, X53CrMnNiN219 (austenitic stainless steel) and X45CrSi93 (martensitic stainless steel) valve steel rods were welded by friction welding. The welded joint was then heat treated at 760 ◦C for 60 min. Mechanical properties of the welded and heat treated samples were identified by means of micro-hardness and tensile tests. Microstructure of the weld and the fracture surface of the tension samples were investigated by optical and scanning electron microscopies. Fractographic evaluations were also performed by using scanning electron microscopy. According to the findings, due to the higher thermal conductivity and lower strength of the martensitic stainless steel, a larger upset and a broader heat affected zone are observed in the martensitic side. Furthermore, formation of non-tempered martensite with the maximum hardness of 880 HV in the heat affected zone (HAZ) of the martensitic stainless steel side makes the as-welded material susceptible to brittle fracture as detected by fractographic examinations. Nevertheless, a successful transition from brittle to ductile behavior is observed by the post-weld heat treatment at 760 ◦C for 60 min.

1-Introduction

Several situations in industrial practices require the joining of dissimilar materials. The joining of dissimilar metals generally faces more challenges compared to similar metals. This is due to the differences in physical, mechanical and metallurgical properties of the parent metals to be joined. On the other hand, in order to take full advantage of the properties of different metals it is necessary to produce high quality joints between them [1]. Austenitic and martensitic stainless steels are the two main groups of stainless steels which are widely used in various industries. The corrosion resistance of martensitic stainless steel (MSS) is less than that of other classes of stainless steels due to lower chromium and higher carbon contents. These steels can be employed when high strength and atmospheric corrosion resistance are required [2]. On the other hand, austenitic stainless steels (ASS) usually offer an excellent combination of resistance to high temperature oxidation, thermal stability, toughness and weldability [3]. X53CrMnNiN219 austenitic stainless steel and X45CrSi93 martensitic stainless steel are normally used to manufacture engine exhaust valve head and stem, respectively. Contrary to the valve stem, the valve head is in direct contact with the burning flame in engines and may

* Corresponding author:
E-mail: khgheisari@scu.ac.ir, khalil.gheisari@yahoo.com

experience a higher temperature than the valve stem [4]. In order to combine the advantages of the aforementioned steels in the engine exhaust valves (i.e., superior creep strength and oxidation resistance of X53CrMnNiN219 austenitic stainless steel and high strength and excellent atmospheric corrosion resistance of X45CrSi93 martensitic stainless steel), a suitable type of welding must be chosen. Recently, more attention has been paid to the solid state welding processes owing to their interesting advantages over the fusion welding processes. The friction welding (FW) method is one of the solid state processes which is well known for high material saving, low production time, low heat input and joining of dissimilar materials. In addition, this process can be used for joining a variety of shapes such as rod to rod, rod to plate, etc. [5-8]. In the friction welding process, frictional heat is generated on the rubbing surfaces to raise the temperature at the interface higher enough to cause the two surfaces to be forged together at high pressure [9, 10]. Microstructural aspects and mechanical properties of the joints can be seriously affected by friction welding parameters including friction pressure, forging pressure, friction time and rotational speed; hence, several attempts have been made to optimize these parameters [11, 12].

There has been several published works on the friction welding of the dissimilar joints. Most of these studies focused on the friction welding of stainless steels to carbon steels, in which the relationship between the properties and welding parameters was usually investigated [13-16]. In spite of the importance of the welded joints between X53CrMnNiN219 austenitic stainless steel and X45CrSi93 martensitic stainless steel in the automobile industry, very few detailed investigations considered their joint microstructure and mechanical properties. Thus, further studies are of vital importance to further develop and to expand the industrial application of these materials.

In this research, X53CrMnNiN219 austenitic stainless steel was jointed to X45CrSi93 martensitic stainless steel by friction welding and subsequent heat treatment. Microstructure and mechanical properties in different regions of the weld are investigated in detail. Regarding the fact that the above mentioned materials are widely used in the automobile industry, this work has considerable industrial attractions.

2- Experimental procedure

The parent metals employed in this study are DIN X53CrMnNiN219 austenitic stainless steel (close to AISI S21900) and DIN X45CrSi93 martensitic stainless steel (AISI S65007). Chemical composition and mechanical properties of these alloys are given in Tables 1 and 2, respectively. The austenitic stainless steel was annealed at 950 °C for 2 hours and then water cooled, leading to the microstructure of austenitic grains and some dispersed carbides in the grain boundaries. The martensitic stainless steel was in a quenching and tempering state (1000-1050 °C, oil quenching; 760 °C for 60 min, oil tempering), leading to a microstructure of tempered sorbite.

The work-pieces in the form of rods of 8 mm in diameter were welded by an industrial continuous drive friction welding machine shown in Fig. 1 (manufactured by Gatwick Technologies Ltd) at a rotation speed of 3000 rpm, a friction pressure of 2413 Pa, a forging pressure of 5860 Pa and a welding time of 6.5 s. After welding, the samples were cooled in air. In order to investigate the effect of heat treatment, one group of the samples was heat treated at 760 °C for 60 min followed by air cooling to room temperature.

The axial cross-section of the joint was obtained by electrospark wire-electrode cutting. The polished cross section was etched for microstructural examinations. The joint microstructure and fracture surfaces were studied by an optical microscope (OM, Olympus BH2-UMA) and a scanning electron microscope (SEM, Philips XL30) coupled with dispersive X-ray spectrometer (EDS). The joint strength and mechanical properties were determined by means of Vickers microhardness and tensile strength tests. The tensile tests were performed according to the ASTM E8 standard and the micro-hardness values were measured from the weld center to the parent metal using a 200 g load and a 10 s dwell time.

Table 1. Chemical composition of the studied alloys (wt. %)

Material	Fe	C	Si	Mn	Cr	Ni	P	S	N
X53CrMnNiN219	Bal.	0.53	0.2	9.0	21.0	4.0	0.45	0.03	0.4
X45CrSi93	Bal.	0.45	2.9	0.5	9.0	0.5	0.04	0.03	0.0

Table 2. Mechanical properties of the used alloys

Material	Yield strength (MPa)	Tensile strength (MPa)	Elongation (%)
X53CrMnNiN219	240.9	1130	12.4
X45CrSi93	236.9	981	22

Fig. 1. The industrial friction welding machine used in this study

3- Result and Discussion

3-1- Microstructure before the postweld heat treatment

Fig. 2 shows the microstructure of the as-received alloys. Carbide particles can be obviously seen in both micrographs. The average size of the carbide particles in the austenitic and tempered martensitic stainless steel is about 1 and 0.4 μm, respectively. The EDS analyses of the matrix phase and carbide precipitations in the austenitic steel are illustrated in Fig. 3. It is evident from the figure that the maximum intensity of chromium in the carbide particles increases to a large extent in comparison with the maximum chromium intensity in the austenite phase. With regard to the high Cr/C ratio, the appeared carbides dispersed at the grain boundaries of the austenite matrix may be $(Cr,Fe)_7C_3$ or $(Cr,Fe)_{23}C_6$ or both. Yu et al.[17] and Li et al.[18] reported that the granular carbides distributed in grain boundaries of this steel are $Cr_{23}C_6$. Chromium carbides are hard and wear-resistant [3] and increase the high temperature strength. With respect to the use of this metal at high temperatures, the formation of these

carbides is necessary to give the required strength.

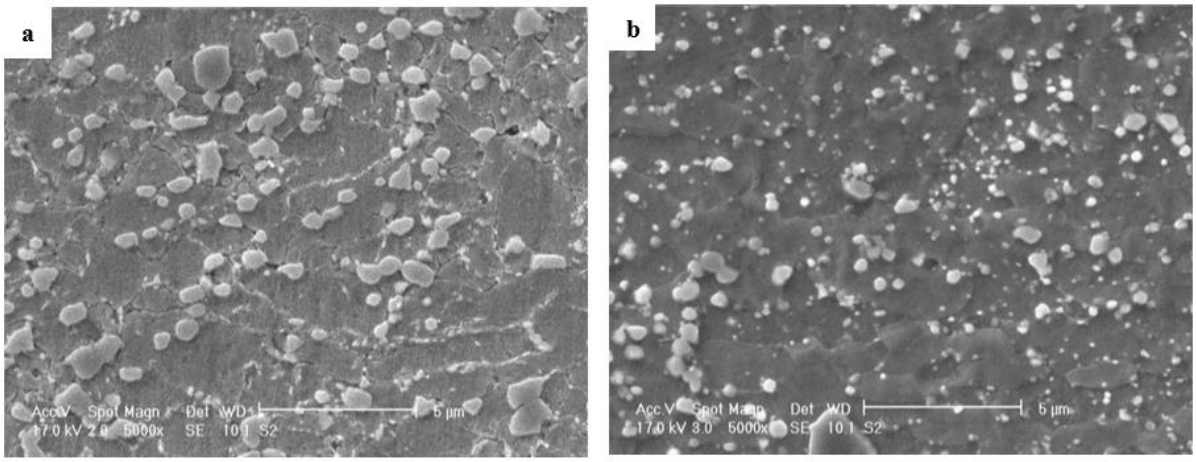

Fig. 2. SEM microstructure of the as-received alloys: Austenitic stainless steel (X53CrMnNiN219) (a) and martensitic stainless steel (X45CrSi93) (b)

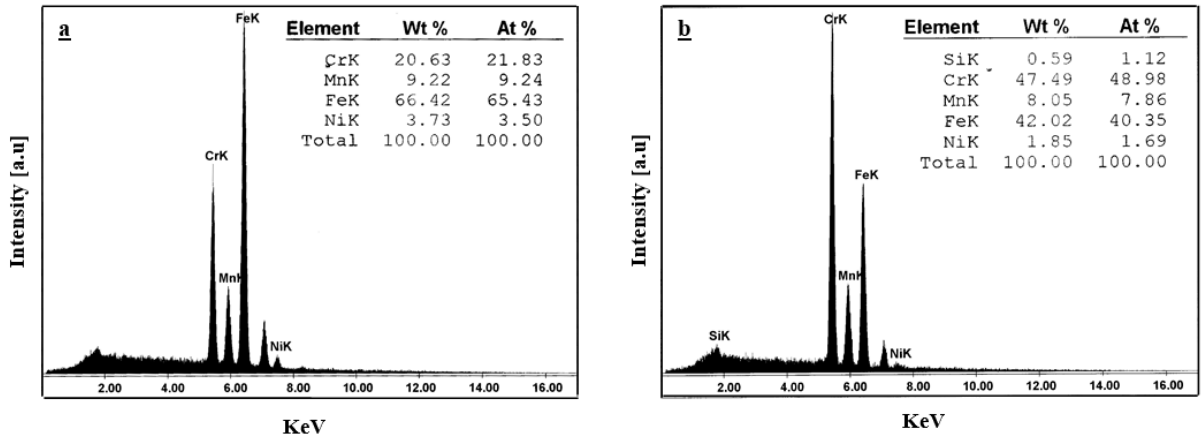

Fig. 3. EDS analysis of the matrix phase (a) and the carbide precipitations (b) in the X53CrMnNiN219 austenitic stainless steel

It should be mentioned that the minimum resolution limit of the EDS analysis in SEM is about 1 µm [19]. On the other hand, the mean carbide particle size in the studied martensitic stainless steel is about 0.4 µm; consequently, the chemical composition of carbide precipitated in X45CrSi93 alloy cannot be accurately determined.

Due to the different physical and mechanical properties of the used austenitic and martensitic stainless steels, asymmetric flashes were observed on both sides of the weld interface. Fig. 4 depicts the schematic diagram of plasticized zones around the weld interface. This figure indicates that a larger flash is formed on the side of the X45CrSi93 martensitic stainless steel. This could be attributed to the excessive softening of the X45CrSi93 side under high temperature resulted from friction heat; accordingly, a remarkable upset inside the X45CrSi93 side (near the interface) is formed during the upsetting process of friction welding. Contrary to the X45CrSi93 martensitic stainless steel, the X53CrMnNiN219 austenitic stainless steel has a higher strength at elevated temperatures. Thus, an insignificant upset is observed inside the X53CrMnNiN219 side in comparison with X45CrSi93. This result is consistent with the findings of Li et al. [18] regarding the microstructure of friction welded 21-4N (austenitic stainless steel) to 4Cr9Si2 (martensitic stainless steel) joint. Additionally, an asymmetric plasticized zone has also been observed in other dissimilar welds [20, 21]. It should be mentioned that in the case of dissimilar friction welding of austenitic–ferritic stainless steels reported by Satyanarayana et al. [1], the flash was observed only in the ferritic

stainless steel side and the austenitic stainless steel did not participate in the flash formation, suggesting that the deformation is mainly limited to the ferritic stainless steel side. In addition, their findings indicated that the flash size decreases with decreasing the forging pressure.

Fig. 4. Schematic longitude section of the joint. Asymmetric flashes can be observed on both sides of the weld interface

Microstructure of the austenitic stainless steel side of the welded joint is shown in Fig. 5. In this case, a distinct heat affected zone is obtained. The HAZ grain size is clearly larger than that of the base metal. Extensive plastic deformation and high heat input in the HAZ of X53CrMnNiN219, i.e. the upset zone, leads to elongated grains in this zone. In addition, a secondary friction surface inside X53CrMnNiN219 is observed in Fig. 5. A possible reason for the formation of the secondary surface is the existence of the highest level of temperature inside X53CrMnNiN219 resulted from the lower thermal conductivity of X53CrMnNiN219 compared to X45CrSi93 [18]. The secondary friction surface can be harmful to the properties of the joint and should be avoided by the implementation of desirable welding process variables or subsequent heat treatment.

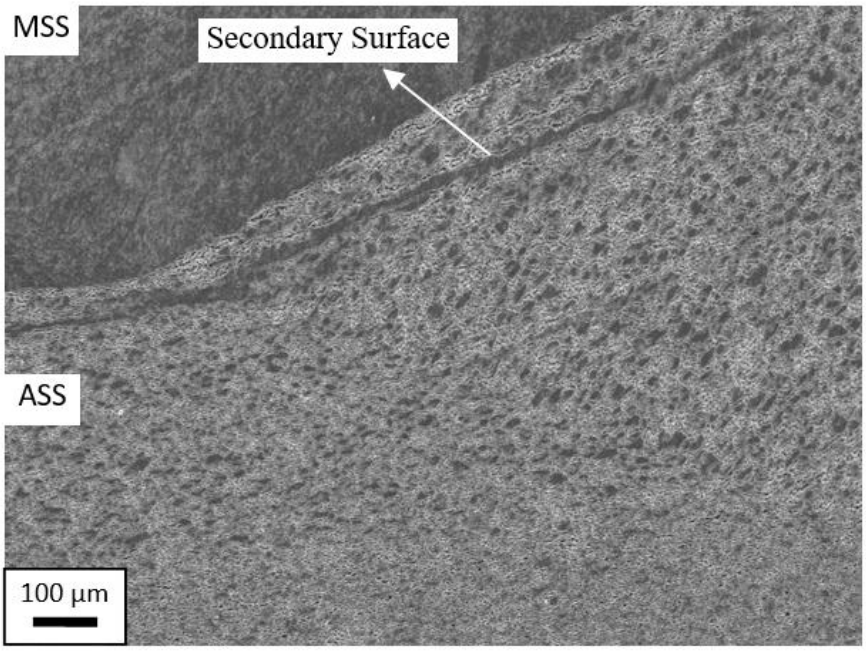

Fig. 5. SEM micrograph of the as-welded X53CrMnNiN219 side at the joint interface. The HAZ grain size is clearly larger than that of the base metal

Fig. 6 illustrates the welded microstructure of the HAZ in the martensitic stainless steel side. A narrow region with a thickness of approximately 150 μm can be easily seen in the martensitic stainless steel side adjacent to the joint interface. During the welding process, the temperature in the HAZ increases to the extent that chromium carbides are dissolved and martensite is transformed to austenite. Consequently, an austenitic solid solution with a high level of carbon is formed at elevated temperatures. Because of the high temperate gradient near the joint interface, chromium carbides cannot re-precipitate during cooling; hence, abundant free carbon atoms are left in this area. On the other hand, austenite phase containing a high carbon concentration is transformed to martensite during cooling; therefore, this area becomes susceptible to embrittlement.

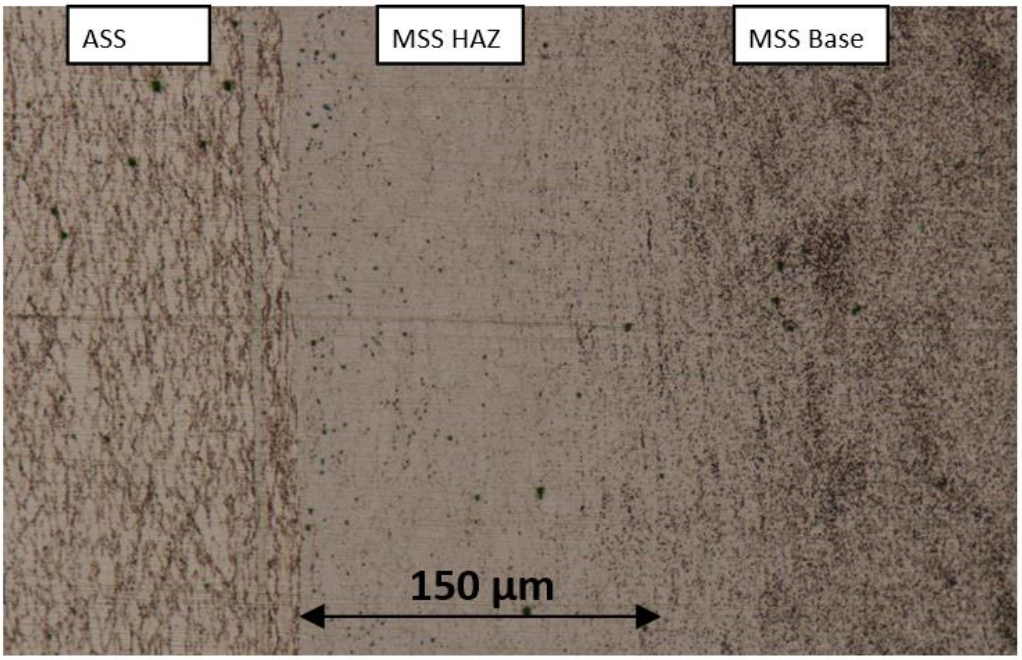

Fig. 6. OM microstructure of the as-welded X45CrSi93 side at the joint interface. A narrow region with a thickness of approximately 150 μm can be observed in the martensitic stainless steel side adjacent to the joint interface

3-2- Microstructure after the postweld heat treatment

Microstructural features in various regions of the austenitic stainless steel side after the post-weld heat treatment for 60 min at 760 °C are indicated in Fig. 7. The HAZ microstructure of the X53CrMnNiN219 alloy after the post-weld heat treatment, especially the grain size, is obviously different from that observed in the welded joint. The smaller grain size is obtained near the joint interface. On the contrary, the large and elongated grains can be seen in the area adjacent to the joint interface (upset zone) of this alloy before annealing (Fig. 5). Grain refinement occurring in the HAZ of the heat treated austenitic stainless steel side is due to the recrystallization phenomenon. During recrystallization, a new set of strain-free, fine and equiaxed grains are replaced by deformed grains [22]. The stored strain energy in the deformed grains of the austenitic stainless steel side (i.e., the upset zone shown in Fig. 5) is the driving force for recrystallization. Furthermore, the reduction of grain size in the recrystallized zone increases the total grain boundary area. As a result, nucleation sites for the carbide precipitation increase and more carbides can precipitate at the grain boundaries, as shown in Fig. 7.

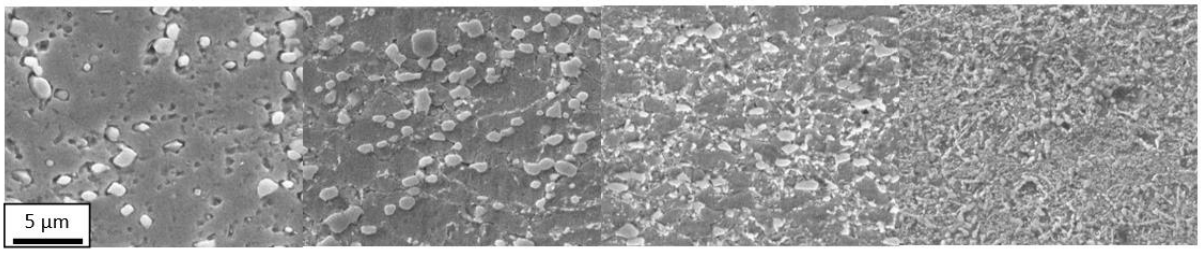

Fig. 7. Microstructure variation from the base metal of the X53CrMnNiN219 alloy to the weld interface (from left to right) after the postweld heat treatment. The grain size is obviously different to that observed in the welded joint.

Microstructure of the martensitic stainless steel side after the post-weld heat treatment at 760 °C is shown in Fig. 8. As can be seen in this figure, the brittle area between the joint interface and the martensitic base metal disappears to some extent. In fact, the postweld heat treatment leads to the formation of tempered martensite. Referring to this figure, microstructure of the tempered martensite consists of extremely small and uniformly dispersed carbide particles embedded within a continuous matrix. The lower carbide density in a narrow region adjacent to the joint interface may be related to the lower carbide nucleation sites resulting from the grain growth which is most likely to occur in this zone.

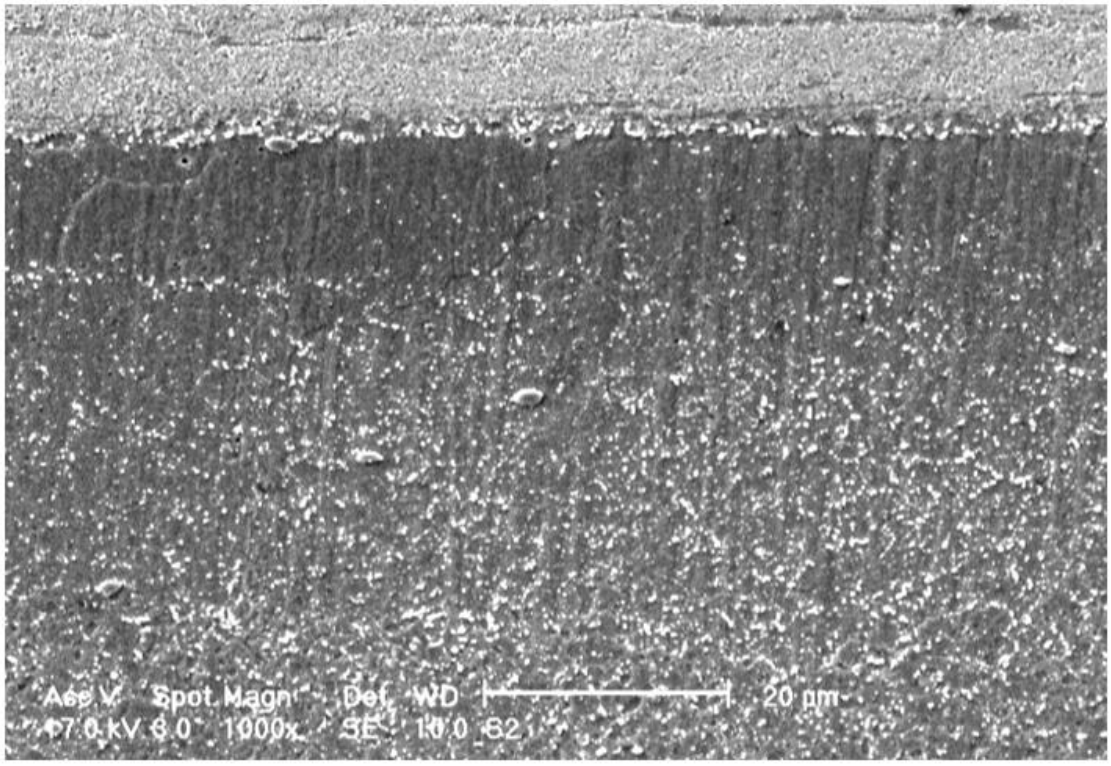

Fig. 8. The HAZ microstructure of the X45CrSi93 alloy after the postweld heat treatment, indicating that the brittle area disappeared through a high-temperature heat treatment process

3-3- Microhardness Test

Figure 9 shows the microhardness distribution in the direction perpendicular to the weld line of the joint cross-section before and after the heat treatment. Microhardness variations in the welded sample, denoted by the solid line, indicate that hardness gradually decreases with increasing the distance from the interface in both sides of the joint. As expected from the microstructural evaluation (Fig. 6), the highest hardness belongs to the HAZ of the martensitic stainless steel which has a non-tempered martensitic structure. Hardness in this region is

about 880 HV (66 HRC) which is comparable to that of the quenched martensite [3]. Therefore, the HAZ microstructure of the martensitic stainless steel is susceptible to brittle fracture and a subsequent heat treatment is required to improve its mechanical properties. Moreover, a slight increase in hardness is also observed in the HAZ of the austenitic stainless steel side, which may have been resulted from the effect of work hardening occurring in the upset zone. Hazlett [23] indicated that the forging pressure in the friction welding process can harden the weld and the HAZ. However, this effect may vary for different materials. The comparison of the hardness variations in the austenitic and martensitic stainless steel sides of the welded joint indicates that a broader HAZ is formed in the martensitic stainless steel side. This is due to the lower strength and higher heat transfer coefficient of the martensitic stainless steel.

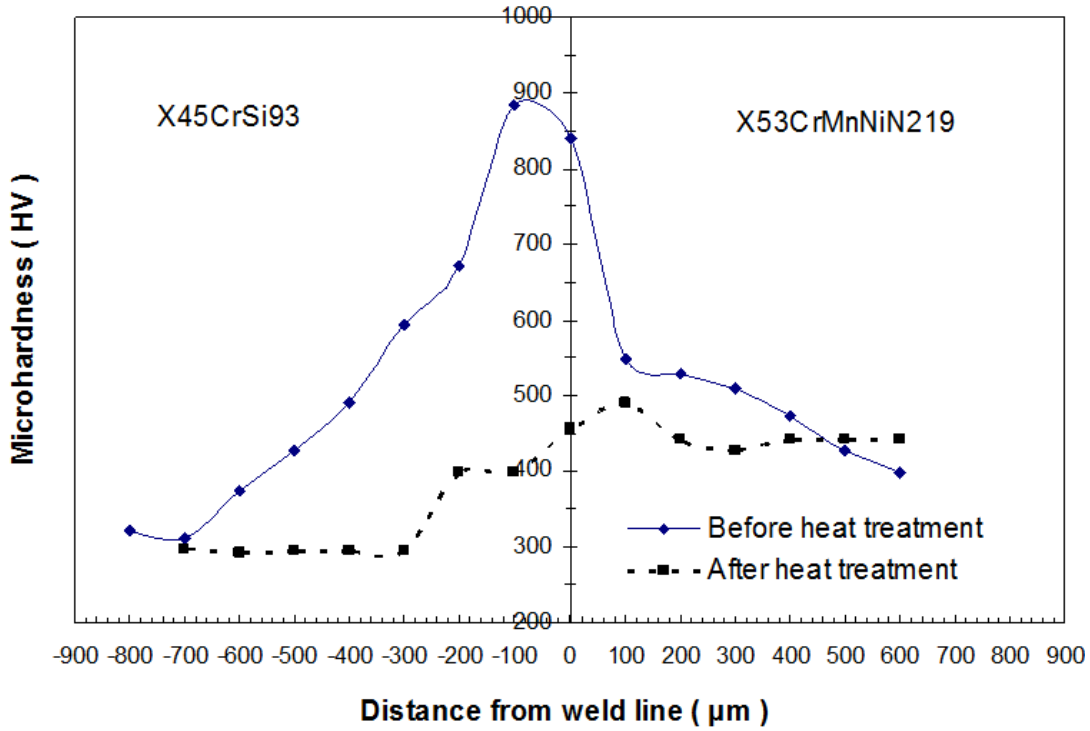

Fig. 9. Microhardness variations along the direction perpendicular to the weld line before and after the postweld heat treatment. The solid and dashed lines represent microhardness variations of the non-annealed and annealed joints, respectively.

The microhardness profile in the post-weld heat treated sample is represented by a dashed line in Fig. 9. The HAZ hardness of the martensitic side decreases significantly during the subsequent heat treatment at 760 °C due to the formation of tempered martensite indicated in Fig. 8. Tempering reduces hardness, increasing the ductility and toughness of this area. Hardness in the HAZ of the austenitic side is also reduced owing to the disappearance of the work-hardening effects during recrystallization. Nevertheless, hardness in the HAZ of the austenitic side is higher than that of the austenitic base metal due to the high density of carbide which precipitated in a narrow region adjacent to the joint interface during recrystallization.

3-4- Tensile Test

As explained in the preceding parts, the post-weld heat treatment improves the mechanical behavior of the friction-welded joint. The tensile test also confirms the previous findings. The appearance of the tensile test specimens after fracture is illustrated in Fig. 10. With regard to this figure, the welded joint represents a brittle fracture without a remarkable plastic deformation, while the heat treated joint indicates a moderately ductile fracture after some necking. As expected from the microstructure and microhardness evaluations, the tensile test sample of the welded joints is broken from the HAZ of the martensitic stainless steel. Furthermore, the heat treated tensile test sample is also broken from the

martensitic side due to the lower tensile strength. The results of the tensile test including tensile strength and elongation values are presented in Table 3. It reveals that the tensile strength of the heat treated sample is slightly higher than that of the X45CrSi93 alloy. The elongation of the heat treated sample is about 22 %, which is similar to the X45CrSi93 alloy and is significantly higher than that of the as-welded sample. The improvement of mechanical properties of the heat treated joint can be ascribed to the microstructure variations. In the as-welded sample, the martensitic transformation is microscopically localized in the HAZ of the martensitic stainless steel. It is well-know that the martensitic structure is so brittle that it cannot be used for most applications; also, any internal stresses that may have been introduced during cooling have a weakening effect. During the tempering heat treatment, the martensite transforms to the tempered martensite, which consists of extremely small carbide particles embedded within a continuous ferrite matrix. In addition, the internal stresses can be relieved by tempering. It is established that tempering heat treatment enhances ductility and toughness, while the transformed microstructure can be nearly as hard and strong as martensite [22]. As a result, unlike the as-welded sample, the superior mechanical properties of the heat treated sample make it perfectly suitable for application as an exhaust valve.

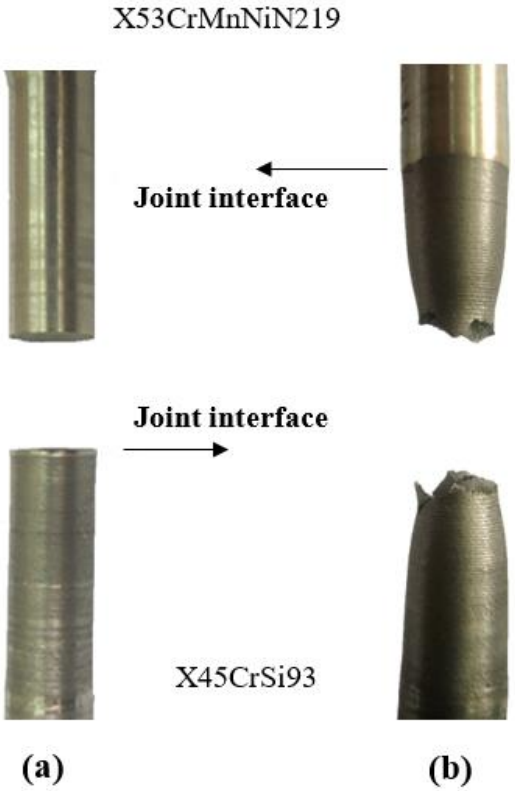

Fig. 10. The appearance of the tensile test specimens after fracture. The brittle fracture in the as-welded sample (a). The ductile fracture in the heat treated sample (b)

Table 3. Mechanical properties of the welded joints at room temperature.

Specimen	Tensile strength(MPa)	Elongation (%)
As-welded sample	943	3
Heat treated sample	1009	22

3-5- Fractographic studies

A more detailed account of the mechanism of fracture resulted from the uniaxial tensile test is given in Fig. 11. The fracture surface of the welded sample reveals a relatively shiny and flat surface which is characteristic of a brittle fracture. In the brittle fracture, if fracture occurs within the grains, the fracture mechanism is called cleavage and if it takes place along the grain boundaries, the fracture mechanism is called brittle intergranular fracture [24]. The fracture surface in Fig. 11a shows the appearance of a cleavage fracture as a low-energy fracture, in which fracture propagates along well-defined low-index crystallographic planes known as cleavage planes [25]. Although a cleavage fracture should be completely flat and featureless, owing to various imperfections such as inclusions and dislocations that affect propagation of cleavage fracture, featureless cleavage is seldom observed. Feather markings (feather pattern) as a fan-shaped array of very fine cleavage steps on a large cleavage facet [25] can be seen on the fracture surface of the as-welded sample, confirming cleavage fracture.

In contrast, the fracture surface of the post weld heat treated sample (Fig 11b) contains numerous semi-spherical dimples which confirm that the fracture is at least moderately ductile. Each dimple is one half of a micro-void formed and then separated during the fracture process [22]. Since the microvoids generally nucleate from the low ductility zones, each dimple is presumably nucleated from a carbide precipitation. The size of the dimple is governed by the number and distribution of microvoids that were nucleated. The relatively small dimples indicate that numerous void-nucleating sites (carbide particles) were activated and the adjacent micro-voids coalesced before having an opportunity to grow to a larger size. Furthermore, Fig 11b exhibits fairly deep conical equiaxed dimples which are expectable when ductile fracture occurred under the condition of uniaxial tensile load [25].

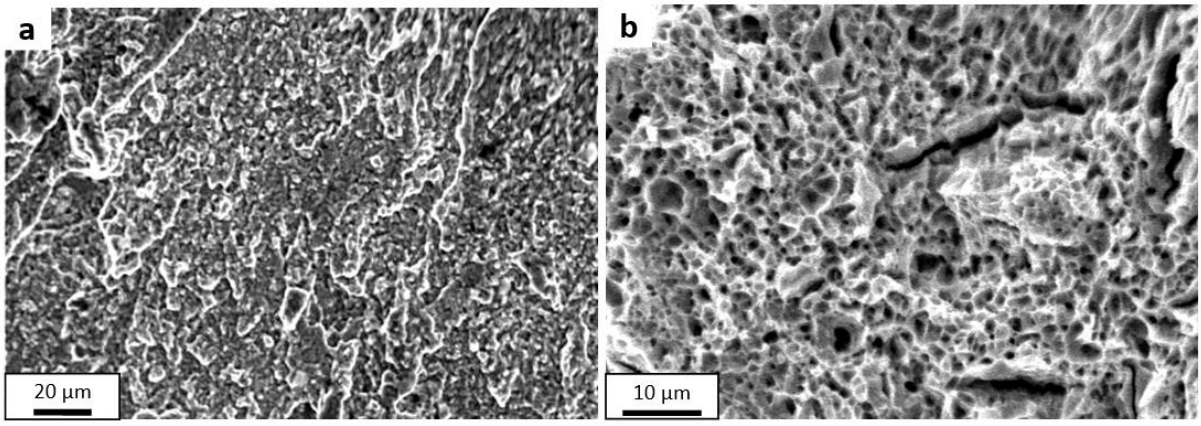

Fig. 11. Fracture surface of the tensile test sample before (a) and after the postweld heat treatment (b), indicating brittle and ductile fracture, respectively

4- Conclusions

Dissimilar metals joining of X53CrMnNiN219 austenitic stainless steel to X45CrSi93 martensitic stainless steel was successfully carried out by the friction welding process and the effects of the post weld heat treatment on the microstructure and mechanical properties were studied. The summary of the important observations is as follows:

(i) The lower strength and the higher thermal conductivity of the X45CrSi93 alloy lead to a larger upset and a broader heat affected zone in the martensitic side, respectively.

(ii) Due to the formation of non-tempered martensite in the HAZ of the X45CrSi93 alloy during welding, the highest microhardness (as high as 880 HV) is obtained in this zone.

(iii) Work hardening occurring in the upset zone of the X45CrSi93 causes a slight increase in the micro-hardness of the HAZ and contributes to recrystallization in the HAZ of the heat treated sample.

(iv) The microhardness profile along the direction perpendicular to the weld line significantly decreases to a lower value by the post-weld heat treatment.

(v) With reference to the tensile test results and the fractographic studies, the brittle fracture is

successfully changes to a ductile fracture after the post-weld heat treatment and all the samples fail in the martensitic stainless steel side.

Acknowledgments

The authors would like to thank Mr. A. Vakiliahrari, Mr. Salimian and Mr. Farhang and their colleagues at Sherkat Toulidi Yadaki Motor Iran (STYM) Company for supporting us in obtaining the data and the samples. In addition, one of the authors (Kh. Gheisari) is grateful to Shahid Chamran University for support of this work.

References

[1] V. V. Satyanarayana, G. M. Reddy, T. Mohandas, "Dissimilar metal friction welding of austenitic–ferritic stainless steels", J. Mater. Process. Technol., Vol. 160, 2005, pp 128-137.

[2] M. Sharifitabar, A. Halvaee, "Resistance upset butt welding of austenitic to martensitic stainless steels", Mater. Design., Vol. 31, 2010, pp 3044–3050.

[3] G. E. Totten, Steel Heat treatment Handbook, 2nd ed, Taylor & Francis, New York, 2006.

[4] Y. Zhu, Z. Zhu, Z. Xiang, Z, Yin, Z. Wu, W. Yan, "Microstructural evolution in 4Cr10Si2Mo at the 4Cr10Si2Mo/Nimonic 80A weld joint by inertia friction welding", J. Alloys. Compd., Vol. 476, 2009, pp 341-347.

[5] R. W. Messler, Joining of Materials and Structures, Elsevier, Burlington, 2004.

[6] J. C. Lippold, D. J. Kotecki, Welding Metallurgy and Weldability of Stainless Steels, John Wily & Sons Inc., New Jersey, 2005.

[7] M. Sahin, "Joining with friction welding of high-speed steel and medium carbon steel", J. Mater. Process. Technol., Vol. 168, 2005, pp 202–210.

[8] M. Asif. M, K. A. Shrikrishana, P. Sathiya, "Finite element modelling and characterization of friction welding on UNS S31803 duplex stainless steel joints", Eng. Sci. Techn. Sci, Int, J., In press.

[9] P. Sathiya, S. Aravindan,A. Noorul Haq, "Some experimental investigations on friction welded stainless steel joints", Mater. Design., Vol. 29, 2008, pp 1099–1109.

[10] P.M. Ajith, B. K. Barik, P. Sathiya, S. Aravindan, "Multiobjective optimization of friction welding of UNS S32205 duplex stainless steel", Def. Technol., In press.

[11] M. Asif, M, K. A. Shrikrishna, P. Sathiya, S. Goel, "The impact of heat input on the strength, toughness, microhardness, microstructure and corrosion aspects of friction welded duplex stainless steel joints", J Manuf. Process., Vol. 18, 2015, pp 92–106.

[12] C. Muralimohan, V. Muthupandi, K. Sivaprasad, "Properties of friction welding titanium-stainless steel joints with a nickel interlayer", P. Mate. Sci., Vol. 5, 2014, pp 1120 – 1129

[13] H. Ma, G. Qin, P. Geng, F. Li, B. Fu, X. Meng, "Microstructure characterization and properties of carbon steel to stainless steel dissimilar metals joint made by friction welding**,** Mater. Design., In press.

[14] M. Hong, Q. Guoliang, G. Peihao, L. Fei, M. Xiangmeng, F. Banglong, "Effect of post-weld heat treatment on friction welded joint of carbon steel to stainless steel", J. Mater. Process. Technol., In press.

[15] N. Arivazhagan, S. Narayanan, S. Singh, S. Prakash, G.M. Reddy, "High temperature corrosion studies on friction welded low alloy steel and stainless steel in air and molten salt environment at 650 ºC", Mater. Design., Vol. 34, 2012, pp 459–468

[16] R. Paventhan, P. R. Lakshminarayanan, V. Balasubramanian, "Optimization of Friction Welding Process Parameters for Joining Carbon Steel and Stainless Steel", J. Iron. Steel. Res. Int., Vol. 19(1), 2012, pp 66-71.

[17] Z. W. Yu, X. L. Xu, "Failure analysis and metallurgical investigation of diesel engine exhaust valves", Eng. Fail. Anal., Vol. 13, 2009, pp 673–682.

[18] W. Y. Li, M. Yu, J. Li, G. Zhang, S. Wang, "Characterizations of 21-4N to 4Cr9Si2 stainless steel dissimilar joint bonded by electric-resistance-heat-aided friction welding", Mater. Design., Vol. 30, 2009, pp 4230–4235.

[19] P. J. Goodhew, J. Humphreys, R. Beanland, Electron Microscopy and Analysis, Taylor & Francis, London, 2001.

[20] S. D. Meshram, T. Mohandas, G. M. Reddy, "Friction welding of dissimilar pure metals", J. Mater. Process. Technol., Vol. 184, 2007, pp 330–337.

[21] M. Sahin, "Joining of stainless-steel and aluminium materials by friction welding", Int. J. Adv. Manuf. Technol., Vol. 41, 2009, pp 487–497.

[22] W. D. Callister, Jr, Fundamentals of Materials Science and Engineering. 7th ed, John Wiley & Sons, New York, 2007.
[23] T. H. Hazlett, "Properties of friction welded plain carbon and low alloy steels", Weld. J., Vol. 41(2), 1962, pp 49s–52s.
[24] T. H. Courtney, Mechanical Behavior of Materials. McGraw-Hill, New York, 1990.
[25] ASM Handbook, Fractography, Vol 12, ASM International, 1992.